Corrosion Resistance of 304L SS Spray Coated with Zirconia Nanoparticles

A Uma Maheswari, M Sivakumar, N Indhumathi and Sreedevi R Mohan

Department of Sciences
Amrita School of Engineering, Coimbatore
Amrita Vishwa Vidyapeetham
Amrita University India– 641 112

Email: m_sivakumar@cb.amrita.edu

Abstract. Influence of substrate temperature on corrosion (in 3.5% NaCl) and wear resistance of nanostructured zirconia thin film coated 304L SS substrates are studied by electrochemical and nano-indentation methods. This analysis shows 304L SS substrate spray coated with nanostructured zirconia at substrate temperature closer to the boiling point of the spray solvent ethanol exhibited good corrosion and wear resistance behaviour. This is because of the compressive stress developed during film fabrication at lower substrate temperature (~50 °C) and hence constrains the indentation plasticity, which leads to higher indentation load than the bare 304L SS.
Key words: Zirconia nanoparticles, Spray coating, Corrosion resistance

1. Introduction

Corrosion is one of the most serious problems faced by industries. Metals normally corrode on exposure to environment and lose its useful properties. Consequently, metal components used in industries have to be repaired or replaced constantly. Though corrosion is inevitable, the rate of corrosion of metals can be reduced by proper choice of material combination [1], using corrosion inhibitors [2] or by surface modification [3] and protective coatings [4]. For instance, stainless steel is widely used for making oil field valves, chemical process equipment, aircraft fittings, fasteners, pump shafts, compressor impeller, nuclear reactor components, gears, paper mill equipment etc., because of its excellent mechanical and corrosion resistance properties. However, in chloride environments at elevated temperatures, austenitic stainless steels are prone to intergranular corrosion due to precipitation of chromium as chromium carbide ($Cr_{23}C_6$) at grain boundaries. This process of precipitation requires large amount of chromium and hence the chromium from the adjacent region diffuse resulting in the formation of chromium-depleted zone. This zone is anodic to the unaffected grains and consequently becomes a preferential site for corrosion attack or crack propagation under tensile stress.

Presently various coating techniques such as oxidation of an evaporated metal film [5, 6], reactive and non-reactive sputtering techniques [7], chemical vapor deposition [8], physical vapour deposition [9] and sol-gel coating [10] are employed to fabricate surface protective coatings for ferrous and non-ferrous alloys. Nevertheless, fabrication of nanocomposite coatings with required proportion of nanostructures like nanoparticles and nanorods of other elements by the above

techniques is quite difficult. Spray technique can overcome the above difficulties and it too provides good adhesion between the coated film and substrate. Spray technique offers the most attractive way for thin film coatings of materials such as ceramic, inorganic oxide, noble metals, metal oxides and spinel oxides [11]. Thin film coatings with oxides of Mg, Ni, Zn, Ti and Zr materials using spray technique is investigated for corrosion and wear resistance of steel [12]. In conventional spray coatings, the cracks propagate through "splat boundaries" which mark the boundary between the materials deposited from the spray solvent. However, in the case of films fabricated using nanostructures, the cracks do not propagate along the "splat boundaries" but propagate through the nanostructures and ends within the grain boundary region. In this context, the present work aim to improve the corrosion resistance of 304L stainless steel (SS) surface in 3.5% NaCl by coating its surface with nanostructured zirconia thin film. Since substrate temperature greatly influence the adhesion and mechanical properties, the films are fabricated at substrate temperature 50 and 150 °C.

2. Experimental methods

2.1. Synthesis of surface modified zirconia nanoparticle

Zirconia nanoparticles for thin film fabrication are synthesized through arrested chemical precipitation method. In this method, tetragonal dominant zirconia nanoparticles are obtained by slow hydrolysis of polyvinylpyrrolidone (PVP) stabilized zirconia tetramers on adding weak alkaline mineralizer NH_4OH [13, 14]. For thin film deposition, the as-synthesized zirconia nanoparticles should have better dispersion stability in spray solvent. For high degree of dispersion stability, the surface of as-synthesized zirconia nanoparticles is modified by silane. Surface modification of zirconia nanoparticles is done by taking 0.8 g of as-synthesized nanocrystals dried in hot air oven for 1 h at 120 °C. The dried sample is grinded and then dispersed in 3 ml acetone by stirring at 300 rpm for 1 h at ambient temperature. Further, the solution is ultrasonicated for 20 min. About 50 wt% of 2- Glycoxy Propyl Tri Methoxy Silane (GPTMS) is added drop wise to the dispersed solution and stirred for 24 h at ambient temperature. To remove impurities, the precipitate is centrifuged at 5000 rpm with acetone for 5 minutes and this is done for three times. Finally, the precipitate is dried in oven at 50 °C for 48 h to obtain surface modified nanoparticles.

2.2. Stabilization of surface modified nanocrystals in spray solvent

The dispersion stability of surface modified zirconia nanoparticles in spray solvent is analyzed by measuring zeta potential (zeta analyzer Horiba, SZ-100). For high degree of stability, the potential should be between +25 mV and -25 mV. ZrO_2 nanoparticles of 0.01 g is dispersed in 15 ml of spay solvent (ethanol + polyvinyl alcohol + polyacrylic acid) and ultrasonicated in bath sonicator for 30 minutes. Then the feedstock (nanoparticles + spray solvent) is kept aside for 20 minutes and stability is measured by injecting a small amount (~ 4 ml) of suspension in to electrode cell. The mean zeta potential of surface modified zirconia nanoparticles is 2.8 mV and hence this confirms the stability of silane modified zirconia nanoparticles in spray solvent.

2.3. Deposition of nanostructured zirconia thin films on 304L stainless steel (SS)

Nanostructured zirconia thin film is deposited by spraying the feedstock (solvent + surface modified zirconia nanoparticles) on SS substrates through syringe pump using spray coating unit (Holmarc Opto-Mechatronics Pvt. Ltd.). The elemental composition (in wt %) of SS substrates are Fe (69.2), C(0.02), Si(0.34), Mn (1.452), P(0.011), S (0.026), Cr (18.87), Mo (0.325), Ni (9.241), Cu (0.398), Nb (0.014), Ti (0.019) and V (0.082). The dispensing rate and speed of syringe pump during coating is controlled precisely by PC based automation. The substrate temperature is controlled independently using a thermocouple set up. Prior to coating, SS substrates are degreased and for removing dirt from surface the samples are sonicated five minutes each in ethanol followed by acetone. Then the sample's surfaces are etched by dipping in acid solution (mixture of 2.5 % H_2SO_4 and 8% HNO_3) for 1 minute. The etched samples are thoroughly rinsed with distilled water for acid removing and finally immersed in distilled water. Further, to improve the adhesion between thin films and sample surface, a layer of silane is coated by dipping sample in 0.25% GPTMS solution for five minutes. For uniform spreading

of silane the samples are kept at an inclination of 30°. The coated silane is cured by keeping samples in oven at 110 °C for 10 minutes. The samples are then rinsed in ethanol to remove excess silane and air dried. The thin films, is fabricated at substrate temperatures 50 and 150 °C and they are designated as Za and Zb respectively. The parameters used for thin film deposition is given in table 1. The spray-coated samples are annealed at 250 °C for 1 hr. The thickness of the coated films is determined using NanoMap PS and found to be 14 ± 3 μm.

Table 1. Spray parameters used for thin film deposition on 304L SS

Deposition parameters	
Feedstock	Nanoparticles, ethanol, PVA, PAA
Amount of zirconia nanoparticles (g)	0.01
Volume of solvent (ml)	Ethanol =12, PVA = 1.5, PAA=1.5
Flow rate (μl/min)	1000
Spray head speed (mm/sec)	x-axis: 50; y-axis: 2
Coating time (min)	22 minutes for 50 runs (syringe pump)
Pressure (bar)	1.4
Substrate temperature (° C)	50, 150
Distance between substrate and syringe (cm)	12
Spray syringe needle diameter (cm)	0.07

2.4. Characterization techniques

The structural analysis of surface modified zirconia nanoparticles and thin films is carried using X-ray diffractometer (PANalytical X' Pert PRO MRD PW3040). The X-ray diffractogram of thin films are recorded using collimated beam geometry. In this geometry parallel beam of Cu Kα radiations are obtained by a parabolic X-ray mirror and directed to the sample under study. The diffracted X-ray radiations are recorded over diffraction angles (2θ) ranging from 10 to 90 º in continuous scan mode at 0.02 º / step. The film thickness of nanostructured zirconia thin film is measured by profilometer NanoMap PS. The corrosion resistance of spray coated zirconia thin films on 304L stainless steel substrates is studied from electrochemical measurements (Potentiodymanic polarization scan) using potentiostat CHI660C. This is a three electrode electrochemical cell: coated sample as working electrode (area 0.28 cm^2), Pt as counter electrode and standard Ag/AgCl as reference electrode. The scan rate is 0.01V/s within a range of –1 V to +1 V. Fourier transform infrared spectra (FTIR) of zirconia nanoparticles before and after surface modification, recorded at room temperature on a Thermo Nicolet, iS10 FT-IR spectrometer ranging from 450 to 4000 cm^{-1}.

3. Results and discussion

3.1. Structural analysis of as-synthesized and surface modified zirconia nanoparticles

Structure of zirconia nanoparticles has significant influence on corrosion resistance of their protective coatings [15]. Figure 1 shows X-ray diffractogram of as-synthesized and surface modified zirconia nanoparticles with predominant tetragonal peaks at 2θ values 29.9, 34.8, 50.1, 59.9 and 81.8 ° corresponding to diffraction from (101), (110), (200), (311) and (331) lattice planes. The spectrum of surface modified nanoparticles also exhibit prominent peaks corresponds to monoclinic phase due to diffraction from planes (-111) and (111). The tetragonal and monoclinic content determines the residual stress of nanoparticles which strongly influences the porosity and hence the corrosion resistance of samples [16]. The percentage of monoclinic content in as-synthesized and surface modified zirconia nanoparticles is analysed using the expression [17]:

$$f_m = \frac{I_m(111)}{I_m(111)+I_t(111)}, \quad (1)$$

where $I_m(111)$ and $I_t(101)$ are the area under (111) and (101) planes of monoclinic and tetragonal phases respectively obtained using Gaussian curve fitting. The monoclinic content of as-synthesized and surface modified zirconia nanoparticles is found to be ~ 24% and ~ 31% respectively.

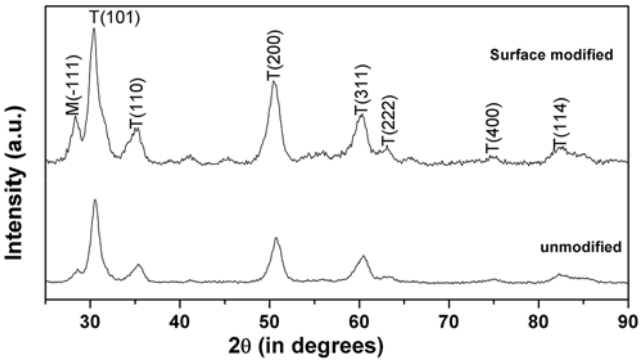

Figure 1. XRD of a) as-synthesized, (b) surface modified ZrO_2 nanoparticles

The FTIR spectra of as-synthesized and surface modified zirconia nanoparticles are shown in figure 2. Both samples showed vibrational band at 2800 - 3000 cm^{-1} and ~ 3400 cm^{-1} corresponding to stretching of C-H bond and hydroxyl ions. The absorption band at 3400 cm^{-1} for as-synthesized sample is stronger than that of modified one. Only surface modified nanoparticles exhibited absorption bands in the range of 1000 - 1200 cm^{-1} attributed to silane bonding with Zr which confirms the condensation of trialkoxy group of GPTMS with hydroxyl groups of ZrO_2 [18]. This bonding improves the compatibility of zirconia nanoparticles in dispersion media and prevents their agglomeration. Further, FTIR spectrum of surface modified nanoparticles showed vibrational bands at 400-900 cm^{-1} ascribed to Zr-O bond and at 742 cm^{-1} in unmodified nanoparticles.

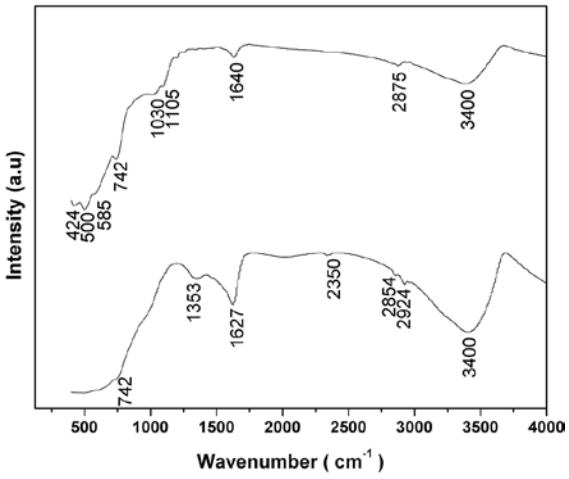

Figure 2. FTIR spectra of as-synthesized and surface modified ZrO_2 nanoparticles

3.2. Structural analysis of spray coated zirconia thin films on stainless steel substrate

Figure 3 shows the X-ray diffractogram of Za and Zb 304L SS samples. The position (2θ) of diffraction peaks corresponding to diffraction from lattice planes and average crystallite size of nanoparticles of the respective planes are tabulated in table 2. The substrate temperature and annealing has caused a significant phase transformation of thin film nanostructures due to residual stress. Consequently, there is slight shift in diffraction peak position with temperature, which determines the nature of lattice dislocations and porosity [19].

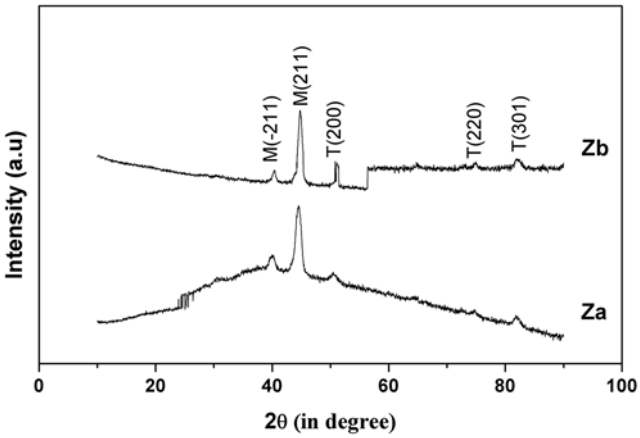

Figure 3. X-ray diffractogram of Za and Zb 304L SS samples

3.3. Microstrain analysis

Stress analysis of thin film coatings for corrosion resistance applications is of great technological importance since they have detrimental or beneficial effect in corrosive environment. Large tensile stress presented in coatings gives rise to cracks, which increases porosity of film and hence fails to protect substrate from corrosion. However, optimum stress is found to inhibit corrosion by resisting crack formation, which is attributed to improved adhesion between coating and substrate. The presence of stress in thin films results in lattice dislocations. Consequently, a change in lattice spacing is observed with respect to that of stress free state of material. The lattice spacing of crystallite planes in nanostructures and thin films depends on their orientation. Hence, direction-dependent strain in films can be estimated from X-ray diffraction data using the relation [20]:

$$\lambda = 2d_{hkl}\sin\theta_h, \qquad (2)$$

which relates lattice spacing d_{hkl} of planes with Laue indices hkl to diffraction angle $2\theta_{hkl}$ and wavelength λ. The d_{hkl} and $2\theta_{hkl}$ are measured from the direction and centroid position of diffraction peaks obtained through Gaussian fit. From data, the elastic strain of planes ε_{hkl} is calculated using the expression:

$$\varepsilon_{hkl} = \frac{d_{hkl}-d_0}{d_0} = \frac{Sin_{\theta_0}}{Sin_{\theta_{hkl}}} \qquad (3)$$

where d_{hkl} is the measured plane spacing of coatings, and d_0 is the standard plane spacing from JCPDS cards 37-1484, 65-2357 (monoclinic zirconia), 14-0534, 17-0923, 42-1164 (tetragonal zirconia) and 27-0997 (cubic zirconia). The residual strain of surface modified zirconia nanoparticles and thin films of Za and Zb samples is calculated and tabulated in Table 2.

Table 2. Microstrain and average crystallite size of Zirconia nanoparticles and thin films Za and Zb

Sample	Peak Indexing	From JCPDS card	2θ	Strain (η)	Size Å
Surface modified ZrO_2	(-111)M	28.175	28.337	-5.72×10^{-3}	94.01
	(111)T	30.308	30.433	-4.11×10^{-3}	62.41
	(110)T	34.855	34.987	-3.77×10^{-3}	60.10
	(220)T	50.596	50.506	1.78×10^{-3}	61.54
	(311)T	60.293	60.186	1.78×10^{-3}	58.99
	(400)T	74.747	74.877	-1.74×10^{-3}	65.08
	(114)T	82.191	82.404	-2.58×10^{-3}	43.89
Za	(-211)m	39.99	40.049	-1.48×10^{-3}	89.51
	(211)M	44.826	44.530	6.66×10^{-3}	90.88
	(220)T	50.596	50.608	-2.41×10^{-4}	93.03
	(400)T	74.747	74.719	3.73×10^{-4}	105.81
	(114)T	82.191	81.968	2.73×10^{-3}	111.41
Zb	(112)M	40.725	40.393	8.22×10^{-3}	89.61
	(211)M	44.826	44.824	4.02×10^{-5}	136.45
	(-122)M	51.193	51.094	1.93×10^{-3}	93.22
	(-113)M	57.168	56.929	4.21×10^{-3}	95.67
	(140)M	75.046	75.061	-1.96×10^{-4}	106.05
	(114)T	82.191	82.110	9.85×10^{-4}	133.83

3.4. SEM analysis of zirconia thin films

SEM micrographs of as-fabricated thin films coated at different substrate temperatures are shown in Fig. 4. It is found that, though crystalline phases of nanostructures are preserved, the substrate temperature caused a significant change in morphology of thin films. The difference is attributed to spreading of polymer (PVA and PAA) at different substrate temperatures. The interaction of surface hydroxyl groups of nanocrystals with hydroxyl groups of polymer increases the thermal stability of polymer and thereby determines the mobility of polymer chains [21] and the film porosity.

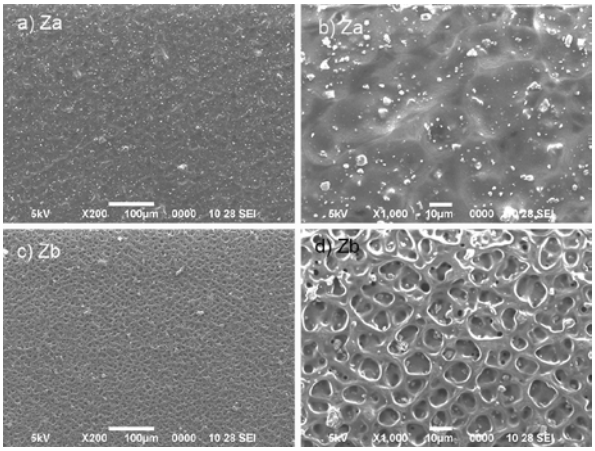

Figure 4. SEM micrographs of a) Za, b) Zb, c) and d) magnified view

3.5. Corrosion analysis from potentiodynamic polarization measurements

The corrosion resistance of coated samples Za and Zb in 3.5% NaCl, is studied by potentiodymanic polarization method. Figure 5 shows the polarization curves (log i vs. potential) recorded for samples coated at substrate temperatures 50 and 100 °C, and bare stainless steel substrate (calcined and un-

calcined). The shift in corrosion potential ΔE (i.e) $\Delta E = \left(E_{corr\ coated\ \ substrate} - E_{corr\ bare}\right)$ of coatings with respect to bare determines the efficiency of coating in protecting 304L SS surface from corrosion. Negative shift of ΔE implies that the oxidation of working electrode takes place at a faster rate and consequently too many electrons is released into electrolyte. These excess electrons shift the potential of working electrode to more negative side and hence speed up cathodic reaction. However, if ΔE is positive, the anodic dissolution rate is less and consequently for positive ΔE there will be a significant reduction in corrosion rate. Figure 5 shows ΔE is positive for Za sample (substrate temperature 50 °C) which indicates lower dissolution rate of coated SS resulting in significant reduction of corrosion current compared to that of bare. This shows that substrate temperature has a significant influence on corrosion resistance of nanostructured zirconia thin film coated 304L SS. The efficiency η of coating in preventing metal from corrosion is calculated using the expression [22, 23]:

$$\eta = \frac{I_{corr\ bare} - I_{corr\ Coated\ \ substrate}}{I_{corr\ bare}} \times 100, \qquad (4)$$

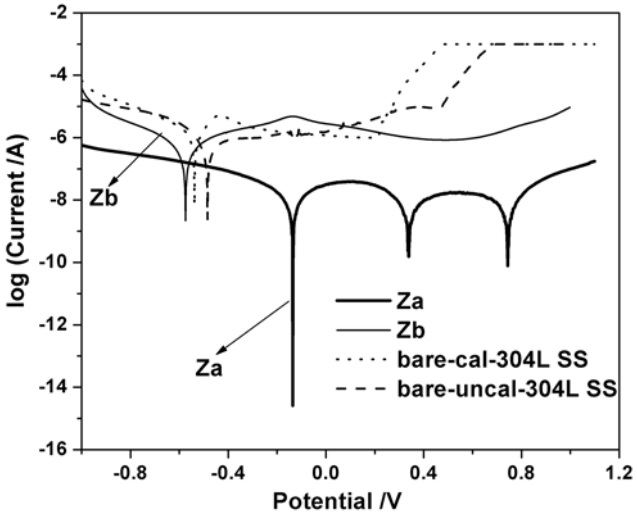

Figure 5. Polarization curves for bare, Za and Zb 304L SS samples

Table 3. Polarization data of bare and nanostructured Zirconia thin film coated 304L SS sample

Sample	Substrate Temp. (°C)	β_c (mV/dec)	β_a (mV/dec)	E_{corr} (V)	I_{corr} (A)	R_p (kΩ)	CRR (mpy)	η (%)
Bare Cal		254	328	-0.538	3.06×10^{-6}	20	3.52	
Bare uncal		168	514	-0.485	9.4×10^{-7}	59	1.08	
			S-ZrO_2					
Za	50	199	254	-0.136	1.4×10^{-8}	3431	0.02	98
Zb	150	188	225	-0.575	4.72×10^{-7}	94	0.54	50

Table 3 shows the substrate temperature plays a significant role during nanostructured thin film fabrication for corrosion resistance applications. This is because at this temperature, the thermal energy will not be sufficient to break the hydrogen bonds formed by surface hydroxyl groups of zirconia nanoparticles with polymer chain. Consequently, at optimum substrate temperature, the mobility of nanoparticles intact with polymer will be moderate and this reduces the probability of crack formation in thin films. Further, optimum tensile stress ascribed to phase transformation from tetragonal to monoclinic results in minimal volume expansion, which avoids the propagation of cracks. During deposition of thin films using nanoparticles by spray technique, direction of crystal growth in film is determined by temperature at the interface of metal oxide and substrate (Figure 3).

Further, while annealing crystallites coalesces causing phase transformation and hence results in significant change in strain. Table 2 shows the strain of surface modified nanoparticles and spray coated samples (Za and Zb). The compressive stress in modified zirconia nanoparticles alone has stabilized the tetragonal phase. However, in thin films a noticeable change in stress of nanocrsytals occurred due to phase transformation from tetragonal to monoclinic caused by substrate temperature and annealing. Moreover, the nature of stress in thin films determines its wear resistance and fracture toughness.

3.6. Mechanical properties of nanostructured zirconia thin films

The electrochemical analysis shows improved corrosion resistance for nanostructured zirconia thin film (substrate temperature 50 and 150 °C) coated 304L SS compared to bare 304L SS. Besides, the coatings should improve its toughness and wear resistance. This can be determined from the nature of residual stress in thin films. Compressive stress improves the adhesion and fatigue strength whereas high tensile stress leads to cracking and fatigue failure of thin film. As a result, the tensile stress in films fails to protect the substrate from corrosion in adverse environment. Consequently, the residual stress has a significant impact on mechanical properties [24], fatigue strength [25], wear and fracture properties [26, 27] of thin films. The toughness and wear-resistance of nanostructured zirconia thin film coated on 304L SS is investigated through Nanoindentation technique. This technique gives information about the mechanical properties of thin films at submicron-or nano-scales [28-30]. Moreover, it gives the details of residual stress in thin films [31]. Nanoindentation experiments were preformed on a Hysitron's TI 700 Ubi 1 Nanoindender through a Berkovich indenter (three sided pyramidal) tip in a continuous stiffness mode. The hardness and Young's modulus of the film and bare substrate is calculated from load (P) versus displacement (h) curve via Oliver and Pharr analysis method and this is a standard method for thin films. The reduced Young's modulus of the film is determined using the expression [32]:

$$E_r = \frac{\sqrt{\pi}}{2\beta} S \frac{1}{\sqrt{A}}, \quad (5)$$

where A- projected area, Contact Stiffness $S = \frac{dP}{dh}$ represents the slope of P versus h at the beginning of the un-loading stage, β - a constant that depends on the geometry of the indenter and its value is 1.034 for Berkovich tip. The projected area A for Berkovich tip is $(\left(24.5 \times {h_c}^2\right))$ where h_c is the contact depth at the maximum load P_{max}. Moreover, the hardness of the film is determined using the expression:

$$H = \frac{P_{max}}{A}. \quad (6)$$

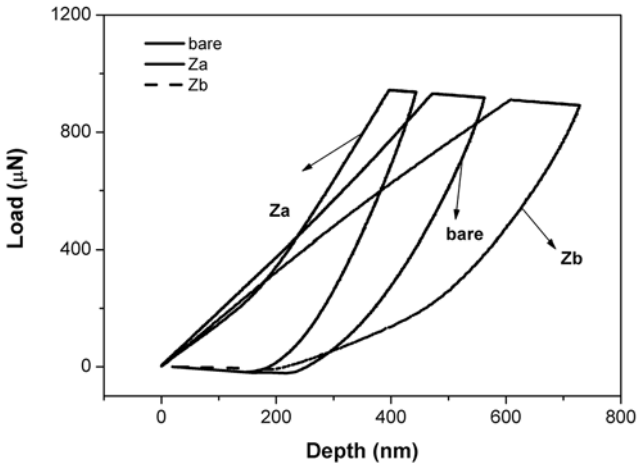

Figure 6. Load (P) versus displacement (h) curve of bare, Za and Zb 304 L SS samples

Figure 6 shows comparison of the P versus h curve of nanostructured zirconia thin film coated 304L SS substrate at substrate temperature 50 and 150 °C with that of the bare 304L SS substrate. Absence

of pop-ins and pop-out during loading and un-loading confirms that there is no crack initiation or propagation. For film with high hardness, the plastic deformation will be less for a given load. The nature of stress in thin films is determined from the loading curve of Figure 6. This portion indicates that the stress in Za is compressive and that of Zb is tensile. The compressive stress in Za limit the plastic deformation that leads to higher indentation load than bare and Zb coated 304L SS substrate. The elongation for a given load is small for Za coated 304L SS substrate. Consequently the hardness and wear resistance of Za coated 304L SS substrate is higher than that of bare and Zb film. Table 4 presents the elastic constant, stiffness, hardness, maximum force and depth, and contact area of indentation of bare, Za and Zb. This data shows that substrate temperature has significant influence on mechanical properties of the spray-coated film. At higher substrate temperature the mechanical properties degraded and the amount of degradation depends on the nature and magnitude of stress.

Table 4. E, H, h_c and S of bare and Za and Zb 304 L SS samples

Sample	Youngs Modulus E	Hardness H	$\frac{H^3}{(E^*)^2}$	Contact Depth h_c	Contact Stiffness S	Max. Force	Max. Depth	Contact Area
	GPa	GPa	MPa	Nm	μN/nm	μN	nm	nm^2
Bare	208	2.03	0.193	429	5	917	562	4.51×10^6
Za	270	2.83	0.310	366	5.5	928	489	3.27×10^6
Zb	117	1.20	0.126	551	3.6	891	729	7.45×10^6

4. Conclusion

Nanostructured zirconia thin film is deposited on 304L SS by spray technique. The corrosion resistance of spray-coated substrate in 3.5% NaCl is studied through potentiodynamic polarization curve. Further, the hardness (H) and effective Young's modulus E* are investigated through nanoindentation. The substrate temperatures greatly influenced the nature of stress in films and consequently it determines the wear and corrosion resistance behaviour of the films. The stress in the films fabricated at lower substrate temperature (< 80 °C) is compressive and this improved its resistance to plastic deformation. Moreover, the compressive stress lowers the probability of crack formation and hence protects the 304L SS from pitting corrosion in 3.5 % NaCl.

Acknowledgement

The authors acknowledge DRDO (ERIP/ER), Government of India, for funding this work.

5. References

[1] Merello R, Botana F J, Botella J, Matres M V and Marcos M 2003 *Corros. Sci.* **45**(5) p. 909.
[2] Vuorinen E, Kálmán E and Focke W 2004 *Surf. Eng.* **20**(4) p. 281.
[3] Gyawali G, Joshi B, Tripathi K, Kim S H and Wohn Lee S 2015 *Surf. Eng.* **31**(9) p. 701.
[4] Aruna S T and Srinivas G 2015 *Surf. Eng.* **31**(9) p. 708.
[5] Chiou Y L, Sow C H, Li G and Ports K A 1990 *Appl. Phys. Lett.* **57**(9) p. 881.
[6] Hass D D, Groves J F and Wadley H N G 2001 *Surf. Coat. Technol.* 146-14785.
[7] Wu W P, Chen Z F and Cong X N 2012 *Surf. Eng.* **28**(8) p. 627.
[8] Liu C, Bi Q, Leyland A and Matthews A 2003 *Corros. Sci.* **45**(6) p. 1257.
[9] Choudhary R K, Mishra P and Hubli R C 2014 *Surf. Eng.* **30**(8) p. 535.
[10] Hubbard K M and Espinoza B F 2000 *Thin Solid Films* **366**(1–2) p. 175.
[11] Ahn S H, Choi Y S, Kim J G and Han J G 2002 *Surf. Coat. Technol.* **150**(2–3) p. 319.
[12] Wang D and Bierwagen G P 2009 *Progress in Organic Coatings* **64**(4) p. 327.
[13] Krishna N G, Thinaharan C, George R P, Parvathavarthini N and Mudali U K 2015 Surf. Eng. **31**(1) p. 39.
[14] Patil P S 1999 *Materials Chemistry and Physics* **59**(3) p. 185.

[15] Bala N, Singh H, Karthikeyan J and Prakash S 2013 *Surf. Eng.* **30**(6) p. 414.
[16] Romero R, Martin F, Ramos-Barrado J R and Leinen D 2010 *Surf. Coat. Technol.* **204**(12–13) p. 2060.
[17] Uma Maheswari A, Saravana Kumar S and Sivakumar M 2013 *J. Nanosci. Nanotechnol.* **13**(6) p. 4409.
[18] Uma Maheswari A, Mohan S R, Saravana Kumar S and Sivakumar M 2014 *Ceram. Int.* **40**(5) p. 6561.
[19] Qin W, Nam C, Li H L and Szpunar J A 2007 *Acta Mater.* **55**(5) p. 1695.
[20] Carvalho J B R, Silva R S, Cesarino I, Machado S A S, Eguiluz K I B, Cavalcanti E B and Salazar-Banda G R 2014 *Ceram. Int.* **40**(8, Part B) p. 13437.
[21] Radoičić Marija B, Šaponjić Zoran V, Marinović-Cincović Milena T, Ahrenkiel Scott P, Bibić Nataša M and Nedeljković Jovan M M 2012 *J. Serb. Chem. Soc.* **77**(5) p. 699.
[22] Luo K, Zhou S, Wu L and Gu G 2008 *Langmuir* **24**(20) p. 11497.
[23] Portinha A, Teixeira V, Carneiro J, Beghi M G, Bottani C E, Franco N, Vassend R, Stoever D and Sequeira A D 2004 Surf. *Coat. Technol.* **188-189**(1-3 SPEC.ISS.) p. 120.
[24] Huang Y C, Chang S Y and Chang C H, 2009 *Thin Solid Films* **517**(17) p. 4857.
[25] Kang H T, Lee Y L and Sun X J 2008 *Mater. Sci. Eng., A* **497**(1–2) p. 37.
[26] Novak S, Kalin M, Lukas P, Anne G, Vleugels J and Van Der Biest O 2007 *J. Eur. Ceram. Soc.* **27**(1) p. 151.
[27] de Portu G, Micele L, Guicciardi S, Fujimura S, Pezzotti G and Sekiguchi Y 2005 *Compos. Sci. Technol.* **65**(10) p. 1501.
[28] Jian S R and Juang J Y 2013 *IEEE Trans. Nanotechnol.* **12**(3) p. 304.
[29] Jian S R, Chang H W, Tseng Y C, Chen P H and Juang, J Y 2013 *Nanoscale Res. Lett.* **8**(1) p. 1.
[30] Jian S R, Ke W C and Juang J Y 2012 *Nanosci. Nanotechnol. Lett.* **4**(6) p. 598.
[31] Zhu L N, Xu B S, Wang H D and Wang C B 2015 *Crit. Rev. Solid State Mater. Sci.* **40**(2) p. 77.
[32] Sneddon I N 1965 *Int. J. Eng. Sci.* **3**(1) p. 47.